Heat and Mass Transfer (2023) 59:95–112
https://doi.org/10.1007/s00231-022-03250-x

ORIGINAL ARTICLE

Correlations to estimate electrical conductivity, thermal conductivity and viscosity of cobalt nanofluid

T. Rajendra Prasad[1] · K. Rama Krishna[2] · K. V. Sharma[3] · C. Naga Bhaskar[4]

Received: 30 October 2021 / Accepted: 12 May 2022 / Published online: 26 May 2022

Abstract
Nanofluid is a better substitute for traditional energy transmission media due to its increased thermal conductivity. Nanofluids present a hitch for researchers in this area due to their lack of long-term uniformity. To improve the homogeneity of the nanofluids, a remarkable mix ratio of Glycerol (G) and Water (W) is determined as the base liquid. Cobalt (Co) nanofluid with a maximum volume concentration of 0.24 per cent (2% weight) was produced with the selected G/W mixture ratio. The Co nanofluid remained homogeneous during the 50-day observation period. The repeated Zeta potential and electrical conductivity tests revealed the nanofluid's unvarying homogeneity during the observed duration. Following the observation time, SEM images also confirmed the homogeneity of Co dispersions. The viscosity and thermal conductivity of nanofluid dispersions are investigated experimentally. A typical thermal conductivity and viscosity enrichment of 19.8% and 16.3% are obtained at 0.24% concentration. Similarly, the augmentation in electrical conductivity was 340 times greater than the base fluid at 0.24% concentration. Within a 10% deviation, empirical correlations are generated for estimating the Viscosity, Electrical and Thermal Conductivities of Co Nanofluids. The heat transfer merit analysis and homogeneity tests on Co dispersions suggest that the chosen G/W blend ratio is an excellent medium for producing stable nanofluids.

Nomenclature

Symbols

C	Specific heat, J/kgK
Co	Cobalt
d	Diameter
k	Thermal conductivity, W/mK
Pr	Prandtl number
T	Temperature, ^{0}C
T_1	Temparature
T	Time, s
w	Weight of nanoparticles

Greek symbols

α	Thermal diffusivity, m^2/s
ϕ	Volume concentration of Nanoparticle
μ	Base fluid Viscosity, cp
ρ	Nanofluid density, kg/m^3
γ	Shear rate, s^{-1}
τ	Shear stress, Pa
σ	Electrical Conductivity, mS/cm
υ_{Br}	Browninan velocity, m/s

Subscripts

bf	Basefluid
nf	Nanofluid
p	Nanoparticle
R	Relative

Abbreviations

BF	Basefluid
EG	Ethylene glycol
G	Glycerol
GON	Graphene Oxide Nanosheets
NP	Nanoparticle
FESEM	Field Emission Scanning Electron Microscope
W	Water

✉ T. Rajendra Prasad
trajendramech@gmail.com

1 Centre for Energy Studies, JNTUH COE, Hyderabad, India

2 Mechanical Engineering, KLEF, Vaddeswaram, Guntur, India

3 Centre for Energy Studies, JNTUH COE, Hyderabad, India

4 Mechanical Engineering, NRI Institute of Technology, Pothavarappadu, Agiripalli, India

1 Introduction

Thermal transport liquids often employed in various fields cannot cope with ever-increasing energy shipping rates. Their low competencies are that their heat conductivities are comparatively low. Research has focused on enhancing heat conductivity in liquids by combining nanometer-sized solid particles in the recent past. Comparatively, liquids have lower thermal conductance than solids. Therefore, suspending sub-micron sized solid particles in liquids can amplify the mixture's overall heat conductance The thermal conductivity of nanofluids rises with concentration and temperature, according to the literature [1]. The random nanoparticle movement and mixing effect of liquid just around the nanoparticles induced due to Brownian motion are acknowledged for enhancements in thermal conductivity [2]. The viscosities of the nano-suspensions were found to be enhancing with concentration and diminish with temperature [3]. However, the relationship between particle diameter and nano-suspension viscosity is unclear. This fact was published in a recent review article by Koca et al. [4]. Li et al. [5] studied thermal conductivities of 25 nm-sized copper particles suspended in the water of concentration 0.1% by weight. They examined the effect of pH and the amount of surfactant used in the nanofluid suspension on enhancement in thermal conductivity. They reported amplification of 10.7% in thermal conductivity by upholding the choicest pH range and surfactant amount of 8.5–9.5 and 0.1% SDBS, respectively. Esfe et al. [6] suspended iron nanoparticles in the water of 37 nm, 71 nm, and 98 nm average diameters and inspected their thermal conductivity and viscosity. They notified that iron nanofluid's thermal conductivity and viscosity increases with concentration and particle diameter. Ghosh et al. [7] measured the thermal conductivity of silver suspended in water. The chemical reduction phenomenon synthesizes the silver particles of a mean size of 45 nm capped with organic surfactants. A significant enhancement in thermal conductivity (> 100%) with the prepared nanofluid, which remained homogenous for 15 days, was observed.

Paul et al. [8] blended gold nanoparticles in the water of varying sizes and concentrations and explored the thermal conductivity of the blends. The researchers prepared the mixtures by chemical reduction process and affirmed arise in thermal conductivity of 48% at 0.00026% volume percentage and particle size of 21 nm. Kim et al. [9] prepared gold nanofluids in water by pulsed laser ablation procedure with concentration range 0.00005–0.018% by volume. The particle size varied between 7.1 – 12.1 nm and claimed an enhancement in thermal conductivity of 9.3% at 0.018% concentration with 7.1 nm particle size with an error of ± 5.4%.In a similar study; Shalkevich et al. [10] blended gold nanofluids in the water of particle size range 2 – 45 nm. The maximum enhancement in thermal conductivity found was only 1.4% at 0.11% concentration and 40 nm size. It is worth noting that reports on properties using identical nano-suspensions show much variance, and they can be due to the difference in stability of the nano-suspensions. Hence, it is essential to determine methods to enhance nanoparticle suspension stability.

Sarojini et al. [11] reported electrical conductivities and influence concerning parameters of water nanofluids suspended with Cu, Cuo and Al_2O_3. The results infer that the electrical conductivity rises with particle volume and declines with the size of the particle. The impact of temperature on the enrichment of electrical conductivity for water-based nanofluids is nominal. Konakanchi et al. [12] examined the electrical conductivity of Al_2O_3, SiO_2 and ZnO nanofluids with 40% propylene glycol mixed with water. The temperature is found to influence the nanofluid's electrical conductivity. The electrical conductance of the tested nanofluids diminishes with particle size and increases with temperature and concentration.

In a significant part of investigations, Water (W) is selected as a base liquid. It is reported that the nanofluid suspension stability is affected by parameters like pH, particle size, viscosity and relative density of the base liquid. The magnification in the viscosity of the base liquid can improve the nanofluid stability [13]. Therefore, a blend of W and Glycerol (G) can improve viscosity instead of W. At 25^0C, G has a boiling point of 290C, a thermal conductivity of 0.281 W/mK and dynamic viscosity of 612cp [14, 15]. For a given nanoparticle, if the G and W blend is employed as a base for nanofluid, the stability can step up.

Furthermore, because G has a more significant difference in freezing and boiling points than water, nanofluids made with G and W mixture base have a wide temperature range in heat transfer applications. The essential chemical and physical characteristics of G are shown in Table 1. An outline of research works on thermophysical properties concerning glycerol or its mixtures as base liquid are shown in Table 2.

Table 1 Properties of Glycerol

Aspect	Remark
Chemical formula	C3H5(OH)3 [14]
Molecular mass	92.09 g/mol [14]
Density, kg/m.^{3}	1261 [14]
Boiling point, ^{0}C	290 [14]
Melting point, ^{0}C	18.2 [14]
Flash point, ^{0}C	160 [14]
Thermal conductivity, W/mK	0.281[15]
Viscosity, cp	612 [15]
pH	Neutral [15]

Table 2 Outline of the investigations done on glycerol as base fluid

BF	NP	D (nm)	ϕ	pH	T (.^{0}C)	Variability in Thermophysical properties	Investigators
G	SiO_2	15–20	0.5–2% (Volume)	10	30–80	Thermal conductivity increased by 11.5% than base fluid at 2% by volume at 60^{0}C, and viscosity reduced by 95% at all concentrations in the 30^0 -80^{0}C temperature range	Akilu et al. [15]
G/EG (60%G by weight)	SiC	45–65	0.3–1% (Volume)	10	15–75	Thermal conductivity increased by 6.8% at 1% volume concentration between 30^0 -60^{0}C, and viscosity reduced by 113% at a concentration of 1% between 30^0 -60^{0}C compared to base liquid	Akilu et al. [16]
G	MgO	21.1, 103.8 and 123.7	0.5–4% (Volume)	-	20–45	Thermal conductivity increased by 19% at 4% by volume than base fluid	Tshimanga et al. [17]
G-W (4:1weight ratio)	GON	0.5-2 µm	0.02–0.1% (Weight)	-	25–45	Thermal conductivity increased by 11.7% than base fluid at 0.1% by volume at 45^{0}C	Ijam et al. [18]
G	Al_2O_3	31, 55 and 134	0.5–4% (Volume)	-	20–45	Thermal conductivity increased by 19.5% than base fluid at 4% by volume at 20^{0}C	Sharifpur et al. [19]
G	Al_2O_3	19, 139 and 160	0–5% (Volume)	-	20–70	Viscosity amplified with the rise in volume fraction diminished with the boost in temperature for all particle sizes, and the small nanoparticles exhibited higher viscosity	Sharifpur et al. [20]
G	Fe_2O_3	26 (mean)	0.125–0.75% (Volume)	-	30–70	Viscosity augmented with volume portion declined with the working temperature	Abareshi et al. [21]

Higher pump capacities in heat transport applications are required if G is used as a base for nano-suspension. G being highly viscous can increase the effective density and subsequent pressure drop [22]. Hence, instead of pure G as a base liquid, a suitable mixture ratio of G/W blend is selected to reduce the pumping capacity with simultaneous enhancement instability of the suspension. It is also to be noted that increasing the content of G in W can decrease in thermal conductivity of the blend, which can reduce heat transfer rates. The present work pinpoints the selection of an optimum blend ratio of G/W as the base for the preparation of Cobalt (Co) nanofluids. Optimal mixture selection of W and G has not yet been documented in the literature. Therefore, this study aims to find the perfect balance between glycerol and water to improve the stability of prepared nanofluid.

Nanofluids are also being studied for cooling electronic components [23, 24]. Different magnetic fields exist in electronic components, across which nanofluid must flow. According to Hatami et al. [25], magnetic fields impact heat transfer rates in nanofluids containing magnetic particles. It is worth investigating the effect of magnetic fields on the heat transfer rate of ferromagnetic cobalt nanofluid in an optimum mixture of glycerol and water. For this reason, magnetic Co nanoparticles were utilized to make nanofluids in this study. There is virtually little study on Co nanofluids in the literature. The first step in assessing nanofluid heat transport is to determine their thermophysical characteristics. This paper attempts to provide data on thermal conductivity and viscosity to further investigate heat transfer characteristics. The values of electrical conductivity are measured which reflects on the nanofluid stability.

Despite the fact that numerous relevant parameters have been investigated by researchers in modeling nanofluid property correlations, generalized correlations that apply to a wide range of nanofluids are still lacking. A shortcoming of existing models, according to Yang et al. [26], is that they are only valid for a limited number of materials in a limited range of applications. The models fail to predict viscosity and thermal conductivity for other nanofluids. While analyzing nanofluid properties, the practical way is still a primary priority. Therefore, regression correlations were developed in this study to theoretically predict thermal conductivity, viscosity and electrical conductivity of produced nanofluids in tested temperature and concentration range. A temperature range of 30 – 70^{0}C and a concentration range of 0.06 – 0.24% is selected.

2 Materials and methods

2.1 Preparation of glycerol-water mixtures

In this study, the selection of ideal blend ratio of Glycerol and Water (G/W) is based on the thermal conductivity and viscosity data of G/W blends of various weight ratios of G. To evaluate of properties of G/W blends, six samples of 50 ml volume holding 0%—50% by weight in steps of 10% of G are prepared. The blends are designated as 0:100 G/W, 10:90 G/W, 20:80 G/W, 30:70 G/W, 40:60 G/W and 50:50 G/W. The experimental data of the properties for all prepared G/W blends is taken.

2.2 Selection of Glycerol and Water (G/W) Ideal Blend Ratio

The thermal conductivity and viscosity of G/W blends are analyzed, and an ideal blend ratio is identified. The data is taken at 30^{0}C. The experimental viscosity data of G/W combinations are compared with the data reported by Cheng [27]. An utmost 7.8% discrepancy is witnessed between the data for the 10:90 G/W solution data. A maximum variation of 9.7% for 40:60 G/W solution is seen when G/W solution is measured thermal conductivity data is compared with data disclosed by Bates [28].

Thermal conductivity decline and viscosity escalate as the amount of glycerol in the mix increases, according to the analysis of measured data. The viscosity of the base liquid influences the nanofluid's suspension stability. The particles move around randomly in the base fluid against viscous drag forces, preventing sediment formation. As a result, the higher viscosity of the base fluid positively impacts the suspension stability of nanofluids. However, increased liquid viscosity is accompanied by increased pumping capacity requirements [22]. So a trade-off between viscosity and pumping capacity requirement is made. The viscosity of the 30:70 G/W blend is 1.86cp, as shown in Table 3. According to these measurements, 30:70 G/W have roughly twice the viscosity of water, enhancing stability compared to water. The increased viscosity enhances relatively low stability for G/W blends with lower G concentrations than 30:70 G/W. The viscosity enhancement grew to higher scales with more excellent concentration blends, requiring more pumping force. When collated to water, the thermal conductivity of the 30:70 G/W blend is 0.491 W/mK as shown in Table 3. Therefore there is not much of a reduction in thermal conductivity. As a result, a 30:70 G/W blend is chosen as the foundation liquid for the fabrication of nanofluids with various cobalt nanoparticle concentrations.

2.3 Preparation and characterization of Cobalt Nanofluids

Cobalt nanofluids with particle loadings of 0.5%, 1%, 1.5% and 2% by weight are intended to be created in a 30:70 G/W blend. The cobalt nanofluids of a mean particle size of 80 nm are procured from Nano Wings Private Limited, India. The nanofluids were made utilizing a two-step physical procedure previously described by several studies [15, 16]. For the ease of comparison with similar works, it is intended to convert weight percentages to volume percentages. The corresponding volume percentages are 0.06%, 0.12%, 0.18%

Table 3 The Viscosity and Thermal conductivity of G/W solutions

Glycerol Percentage	Viscosity Results (cp)			Thermal Conductivity Results (W/mK)		
	Reference Data [27]	Measured Data	% Deviation	Reference Data [28]	Measured Data	% Deviation
0	0.799	0.84	-5.0	0.612	0.626	2.2
10	1.02	1.1	-7.8	0.573	0.533	-7.5
20	1.34	1.29	4.2	0.531	0.484	-9.4
30	1.85	1.86	-0.5	0.489	0.491	-0.4
40	2.7	2.63	2.6	0.452	0.412	-9.7
50	4.22	3.92	7.2	0.418	0.387	-8.0

and 0.24%. The weight percentages of cobalt nanofluids are related to their volume percentages (ϕ), as shown in Eq. (1).

$$\phi = \frac{\left(\frac{w_p}{\rho_p}\right)}{\left(\frac{w_p}{\rho_p}\right) + \left(\frac{w_{bf}}{\rho_{bf}}\right)} \times 100 \tag{1}$$

The nano-powder and liquid base weights were measured using an electronic balance (Model CAS-164, Contech Instruments Limited, India) with a precision of 0.0001 g. Where w_p is the weight of the particle, w_{bf} is the weight of the base liquid, ρ_p is the density of the particle and ρ_{bf} is the density of the base liquid, respectively. Equation (2) is utilized to compute the base liquid's density [22].

$$\rho_{nf} = \phi\rho_p + (1 - \phi)\rho_{bf} \tag{2}$$

No chemical dispersants were used during the preparation of the nanofluids. In order to lengthen suspension stability, ultrasonication and pH control are crucial features of nanofluid production. The sonication of a nanofluid enables the disintegration of large particle clusters, resulting in a near lump-free suspension [15]. Many studies employed sonication to create well-dispersed nanofluids that remained sediment-free for several days [13, 16]. The prepared Co nanofluids were sonicated for one hour in this study to ensure steady suspension. According to Jamshidi et al. [29], one hour of ultrasonic treatment was enough to disaggregate nanoparticles and yield stable nanofluids.

FESEM (Thermo Fisher Scientific, USA) is utilized to analyze the Co nanoparticle shape, size, and dispersion stability. Further zeta potential tests are also conducted to establish the effect of pH on dispersion stability. For FESEM and zeta potential analysis, the 0.24% Co nanofluid is considered. The 0.24% Co nanofluid is selected for FESEM and zeta potential analysis because it has the highest concentration and more possibility of particle clustering and sedimentation. The increased particle number at higher concentrations reduces the distances between the particles, thereby increasing the Vander Waal's forces between them. This phenomenon increases agglomeration and reduces dispersion stability [13, 30]. Krishnan and Nagarajan [31] also claimed about reduced stabilities of nanofluids at higher concentrations due to enhancement in Vander Waal's forces between the nanoparticles. Choudhary et al. [32] also reported that the nanofluid zeta potential reduces with particle volume in the nanofluids.

The image of the 0.24% nanofluid sample taken after 50 days of preparation is carried by FESEM. The FESEM image in Fig. 1(a) manifests that the cobalt particles are nearly globular and well dispersed. From the image, the average diameter of the particles, 80 nm, affirmed by the manufacturer, is in close concurrence. The particle agglomeration is not observed, reaffirming that the nanofluids devised have

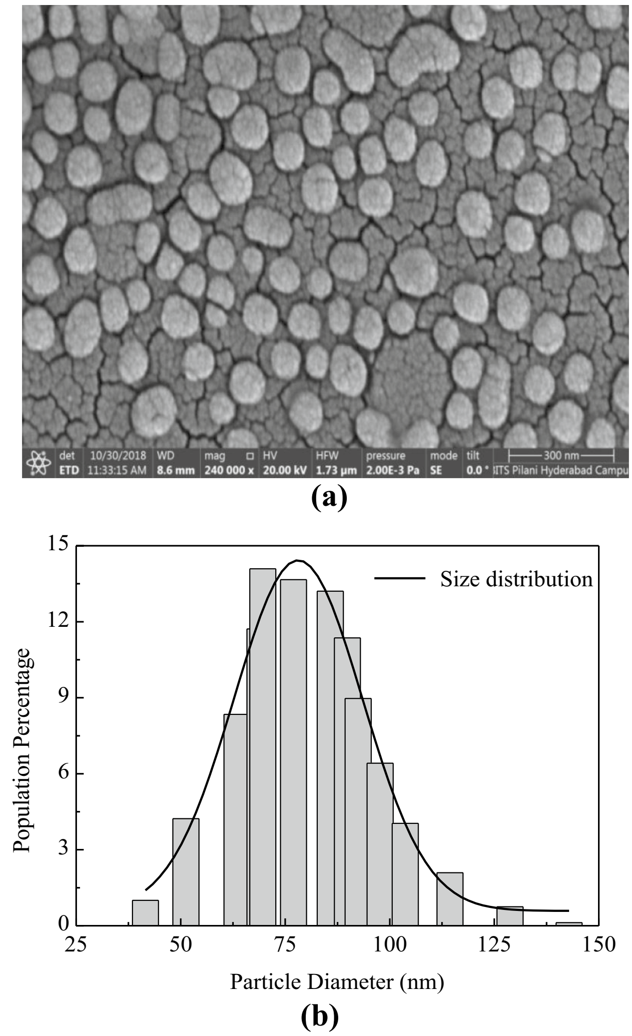

Fig. 1 The **a** FESEM image and **b** Particle size distribution of cobalt nanoparticles

good stability even after 50 days from preparation. In a similar investigation, Hwang et al. [33] used Transmission Electron Microscopy (TEM) to study the aggregation behavior of carbon black and silver nanofluids in different base media. The particle diameter distribution histogram is revealed in Fig. 1(b), which concludes an average particle diameter of about 80 nm for the used Cobalt particles.

2.4 Measurement of thermal conductivity

The thermal conductivity of G/W blends and nanofluids are measured with KD2 Pro thermal properties analyzer (Decagon Devices Inc., USA). KD2 Pro was used by many researchers to measure the thermal conductivity of nanofluids [6, 8, 15–19, 42]. The KD2 Pro gauges the thermal conductivity on par with standards put forth by the American Society for

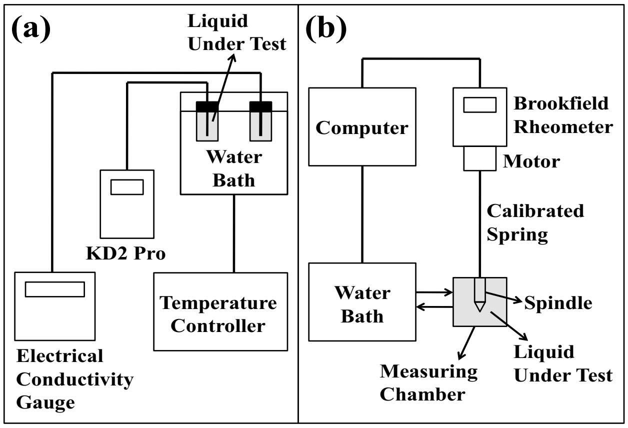

Fig. 2 Procedure for Testing of **a** Thermal Conductivity and Electrical Conductivity **b** Viscosity

Testing and Materials (ASTM) and the Institute of Electrical and Electronics Engineers Standards Association (IEEE-SA) [34]. The device employs a transient line source of heat in measuring thermal properties. The thermal conductivity of test liquid is approximated by response relative to the temperature of the infinite line of heat source exposed to a sudden electric energy pulse. The approximation of the concerned parameters of the device is related as follows:

$$k = \frac{q ln\left(\frac{t_2}{t_1}\right)}{4\pi\left(\Delta T_2 - \Delta T_1\right)} \quad (3)$$

In the above relation, k = thermal conductivity, q = electrical energy pulse/length, ΔT_1, ΔT_2 are temperature variations at time t_1 and t_2, respectively. A cylindrical mono-needle type metal probe called KS-1 of 60 mm long and 1.27 mm thick is utilized as prescribed for liquids. The KS-1 harmonizes the heater with the thermistor to accredit thermal conductivity testing with an exactness of ± 5%. The measuring range of the device is 0.2 – 2 W/mK. The liquid sample under test is filled in a 30 mL glass measuring jar and kept in a temperature-controlled water bath (Ilabot Technologies, Model HPWB5, India). The measuring jar is held in place utilizing a metal stand. An external flexible probe temperature sensor is utilized to check the thermal equilibrium between the water bath and sample. The needle sensor is kept perfectly vertical to arrest any chance of convective errors inside the fluid sample.

Along with KD2 Pro, the whole arrangement is arranged on a table undisturbed to avoid any possible errors caused due to external vibrations. The procedure for conducting tests by KD2 Pro is shown in Fig. 2(a). The random errors associated with the thermal conductivity measurement are minimized by repeating the experiment six times, and the average of all the iterations is considered the final result. The thermal conductivity tests of G/W samples are conducted at a room temperature of 30^0C and compared. The glycerol thermal conductivity data was taken with KD2 Pro and compared data with the publicized values in the literature. The reliability test results of KD2 Pro are shown in Table 4. The maximum percentage deviation in the reliability test is found to be within 3%.

2.5 Measurement of viscosity

The viscosity of G/W blends and nanofluids are measured with Brookfield rheometer (LVDV-III, Brookfield Engineering Inc., USA). Previously, researchers measured the viscosity of nanofluids using a Brookfield rheometer [15, 16, 21]. The Brookfield LVDV-III rheometer is programmable, quantifying shear stress and viscosity under a given range of shear rates. This device operates by a power-driven spindle surrounded by a liquid being tested. A calibrated spring powers the spindle, and the spring slew tests the viscous drag of the solution alongside the spindle. A revolving transducer senses the deflection of the spring. The spindle rotates in a container in which liquid is placed. The speed of the spindle is in the range of 0 to 250 RPM, and the operating temperature range is -100 to 300^0C. A circulating water bath controls the temperature of the liquid sample of 15 ml approximately in the removable measuring container.

The liquid sample is filled in the measuring chamber and reattached to the rheometer. A computer adjusts the required

Table 4 The reliability of Thermal Conductivity testing by KD2 Pro

T, ^{0}C	Thermal Conductivity, W/mK					
	Glycerol			Ethylene Glycol		
	Measured Data	Reported Data [15]	% Deviation	Measured	Reported Data [15]	% Deviation
30	0.282	0.281	0.35	0.255	0.252	1.17
40	0.286	0.282	1.39	0.259	0.254	1.93
50	0.289	0.283	2.07	0.262	0.256	2.29
60	0.291	0.284	2.40	0.266	0.258	3.01

Table 5 The reliability of Viscosity measurement by Brookfield rheometer

T, ^{0}C	Viscosity, cp					
	Glycerol			Ethylene Glycol		
	Measured	Reported [15]	% Deviation	Measured	Reported [15]	% Deviation
30	604.2	598	1.02	13.59	13.42	1.25
40	291.6	283	2.94	9.43	9.2	2.43
50	152.1	148	2.69	6.81	6.63	2.64
60	83.5	81.1	2.87	4.92	4.78	2.84

temperature and shear rate range of the test. The laptop also serves as data acquisition and storage gadget. The procedure for conducting viscosity tests by rheometer is shown in Fig. 2(b). The sample reaches the maximum re-set temperature; the test is conducted in a few minutes. The viscosity data of G/W samples are taken at room temperature of 30^{0}C between the shear rates range of 0 – 200 s^{-1}. Each measurement is repeated six times, and the mean of the outputs is used for the analysis. The reported viscosity data of Glycerol and Ethylene Glycol is utilized to evaluate the reliability of the rheometer, given in Table 5. The maximum percentage deviation in the reliability test is found to be within 3%.

2.6 Measurement of electrical conductivity

A standard probe type electrical conductivity gauge (Tech-Ed Equipment Company, India) is utilized to test the electrical conductivity of Co nanofluids. Previously, various researchers employed ordinary probe type electrical conductivity meters [11, 12, 42]. The liquid sample under test is filled in a 30 mL glass measuring jar and kept in a temperature-controlled water bath (Ilabot Technologies, Model HPWB5, India). The measuring jar is held in place utilizing a metal stand. An external flexible probe temperature sensor checks the thermal equilibrium between the water bath and sample. The procedure for conducting electrical conductivity measurement is revealed in Fig. 2(a). The determination of the electrical conductivity of all the prepared nanofluids on day 1 was undertaken. The electrical conductivity test of 0.24% nanofluid is repeated on day 50 after the trial to check for suspension stability. The gauge is a linear instrument and can be calibrated by the single-point calibration method. Before measuring, the electrical conductivity meter is calibrated by using a 0.1 M (molar) KCl solution whose electrical conductivity is 1.54mS/cm at 30^{0}C [35]. The usage of 0.1 M KCl solution for the calibration process is prescribed by the supplier of the electrical conductivity gauge. The calibration test was conducted five times and found that the deviations were within ± 5%. The calibration test results of the electrical conductivity gauge are shown in Table 6.

2.7 Measurement of zeta potential

The Zeta potential of Co nanofluids is measured by the Nanopartica SZ-100 series (Horiba Scientific, Spain). The Zeta potential reflects electrostatic repulsive forces in-between the suspended particles in the nanofluids, and the repulsive forces are affected by the pH of the nanofluid. There lies a pH value for every nanofluid where zeta potential becomes zero, called Iso-Electric Potential (IEP). Hence, adjusting the pH of the nanofluid shifts the zeta potential aside from the IEP, enhancing the zeta potential, thus ensuring the nanofluid's stability. The Zeta potential above ± 30 mV represents good suspension stability [13, 36]. Hence, it is intended to evaluate the Zeta potentials of Co nanofluid stabilities at various pH values. The 0.24% Co nanofluid is selected for Zeta potential analysis, and the reason for its selection is explained earlier. The nanofluid samples of 5 mL each of 2, 5, 7.5, 9 and 12pH were prepared by mixing tiny droplets of Hydrochloric acid (HCl) and Sodium hydroxide (NaOH).

The initial pH of prepared 0.24% Co nanofluid is 8.6. A small portion of 0.24% Co nanofluid about 10 mL is taken, and the addition of a tiny droplet of concentrated NaOH solution and subsequent stirring made the nanofluid reach 9pH. 5 mL of the nanofluid is stored in a separate glass bottle. The nanofluid is made to reach 12pH by adding a few more droplets of NaOH solution and constant stirring, and 5 mL of it is stored. 15 mL of 0.24% Co nanofluid is again separated to make 5 mL samples of 2, 5 and 7.5pH by

Table 6 The calibration test of the Electrical Conductivity gauge

T, ^{0}C	Electrical Conductivity, mS/cm		
	0.1 M KCl solution		
	Measured	Reported [35]	Deviation
30	1.48	1.54	-4.05
30	1.51	1.54	-1.98
30	1.49	1.54	-3.35
30	1.47	1.54	-4.76
30	1.49	1.54	-3.35

adding tiny droplets of HCl solution. All these 5 mL nanofluid samples are used to measure the Zeta potential. The Zeta potential tests of these samples were conducted on day one and after 50 days of preparation.

3 Results and discussion

3.1 Stability of Co nanofluids

The variation of zeta potential with pH on both iterations is shown in Fig. 3. It is observed from Fig. 3 that the cobalt nanofluids have the highest zeta potential at 7.5pH on both measurement iterations. On Day 1and Day 50, the zeta potentials are 36.2 mV and 32.7 mV, respectively, at 7.5pH, showing a deviation of 9.6%. Moreover, at both measurement iterations, the zeta potential is more than the stability benchmark of 30 mV [13]. Hence, the prepared Co nanofluids are stable for 50 days at 7.5pH. Thus, Cobalt nanofluids at all concentrations are maintained at 7.5pH while measuring the properties to ensure accuracy. Several investigators probed the outcome of pH on measured thermophysical properties. Li et al. [5] also studied the pH influence on measured thermal conductivity. They reported that the Cu-Water nanofluid exhibited higher enrichment in thermal conductivity by maintaining their pH between 8.5 and 9.5.

3.2 Electrical conductivity of cobalt nanofluids

3.2.1 Effect of temperature and concentration on electrical conductivity

The nanofluid samples are tested for their electrical conductivities at different concentrations in the temperature range of 30—70^{0}C, and values are graphically represented in Fig. 4(a). An inspection of Fig. 4(a) indicates that the electrical conductivity of nanofluids improved with 30:70 G/W base liquid. The electrical conductivity of the prepared cobalt nanofluids improved with concentration and temperature. The physiochemical linkages in the nanofluid dispersion like formation electrical double layer (EDL) and the culmination of net charge on particle are considered factors for improving nanofluid's electrical conductivity compared to base liquid [11]. When a nanoparticle is suspended in a base liquid, the charge formation on the particle surface attracts ions of opposite polarity and repels ions of similar polarity. The accumulation of ions of opposite polarity at the particle surface creates a surplus electric potential near the nanoparticle surface. This charged layer is called EDL and constitutes a complex pattern. The formation of charge on nanoparticle surface and EDL

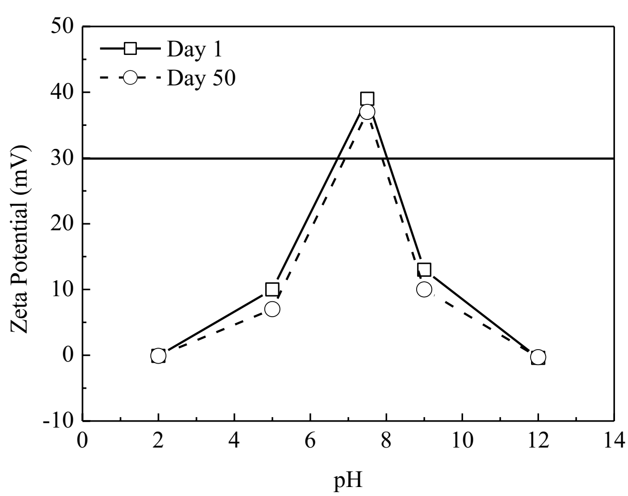

Fig. 3 Variation of Zeta potential with pH

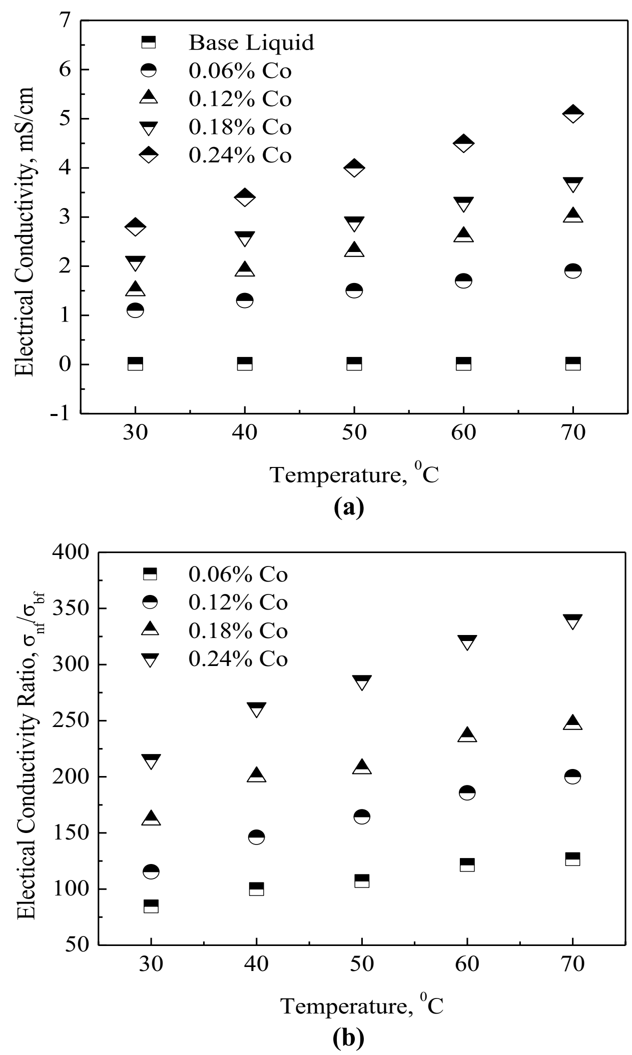

Fig. 4 Variation of **a** Electrical Conductivity and **b** Electrical Conductivity Ratio with Temperature

may be attributed to the improvements in electrical conductivity of nanofluids [37]. The construction of EDL is a positive sign for the suspension stability of the nanofluids, enhancing the movement of nanoparticles in the suspension due to electrophoresis. When nanoparticle concentration increases, it creates enhanced charge carriers, resulting in improved electrical conductivity of nanofluids with concentration [38]. Figure 4(b) shows a significant enrichment of nanofluid electrical conductivity with particle volume. It is also noticed that the electrical conductivity ratios enlarged with temperature but not to the extent observed with concentration, which agrees with the report published by Minea and Luciu [39].

The present trend in improvements of measured cobalt nanofluid electrical conductivities contrasts with Konakanchi et al. [12], claiming that temperature is predominant compared to concentration on electrical conductivity improvements of silica and alumina nanofluids in PG/W base mixture. For instance, the Cobalt nanofluid electrical conductivity ratio increases from 84.6 to 126.7 in the temperature range of 30^0C to 70^0C for 0.06% concentration. But electrical conductivity ratio of cobalt nanofluids increases from 84.6 to 215.4 between the concentrations of 0.06% to 0.24% at 30^0C. The maximum enhancement in the electrical conductivity is found to be 340 times of base liquid at 0.24% concentration and 70^0C. In an analogous study, Baby and Ramaprabhu [40] have shown a maximum improvement of 1400% in electrical conductivity of water-based graphene nanofluids at just 0.03% volume concentration and 25^0C.

3.2.2 Reproducibility of electrical conductivity

Several researchers looked at the repeatability of measured data of nanofluid properties over a specific period to estimate the nanofluid suspension stability. For example, Sadri et al. [41] tested the repeatability of thermal conductivity values of carbon nanotube suspensions over 28 days. Hence, to establish the Cobalt nanofluid stability, the electrical conductivity is measured on Day 1and Day 50 from preparation and the deviation in the values is analyzed. The disparity in electrical conductivity of cobalt nanofluids with time from the first trial is shown in Fig. 5. It is witnessed that the highest deviation in electrical conductivity measured on Day 1 and Day 50 is 4%. The observation of low variation in the measured data reflects a good reproducibility, and hence, the prepared cobalt nanofluids are stable within the tested time frame.

3.3 Thermal conductivity of cobalt nanofluids

3.3.1 Effect of temperature and concentration on thermal conductivity

After analyzing the dispersion stability of prepared cobalt nanofluids, the thermal conductivity is measured on Day 50 of preparation. Thermal conductivity is tested at temperatures

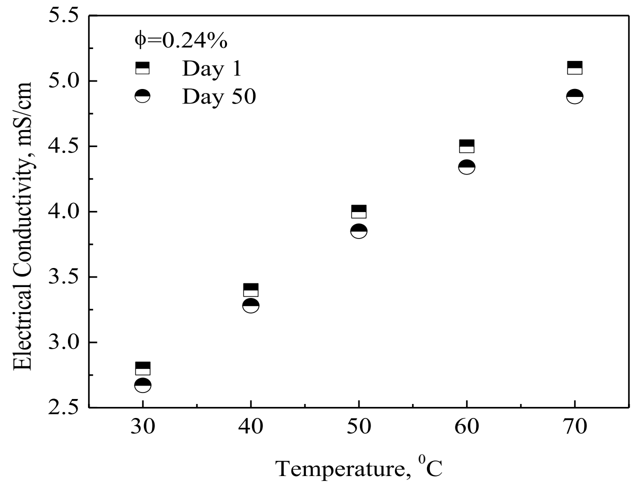

Fig. 5 Variation of electrical conductivity with time

ranging from 30—70^0C. The thermal conductivity of cobalt nanofluids at various temperatures is tested at 7.5 pH. The measurement of nanofluid thermal conductivity was undertaken with KD2 Pro thermal property analyzer. Previous researchers [15, 16, 42] employed the KD2 Pro to assess nanofluid thermal conductivity. The accuracy and validity of the KD2 Pro's experimental results were tested using standard liquids such as water, glycerol, and ethylene glycol, all of which have known thermal conductivity values. Figure 6(a) depicts how the thermal conductivity changes with temperature rise for varying concentrations of cobalt nanoparticles. The nanofluid thermal conductivity is appeared to be more than base liquid. Nanofluid has more excellent thermal conductivity than base liquid because of the existence of a submicron layer of base fluid molecules at the particle surface [8].

Figure 6(b) depicts the wide fluctuation of nanofluid's thermal conductivity ratio (k_{nf}/k_{bf}) about the temperature at various cobalt concentrations. A close examination of Fig. 6(b) reveals that the thermal conductivity ratio improves as concentration and temperature rise. The thermal conductivity of cobalt nanofluid at 0.06% concentration is 0.517 W/mK at 30^0C and 0.585 W/mK at 60^0C, suggesting a 5.5% to 10.3% improvement over base fluid. The maximum concentration of 0.24% results in the largest improvement in nanofluid thermal conductivity of 19.8% at 60^0C. Cobalt nanofluids have thermal conductivities of 0.517 W/mK at 0.06% cobalt concentration and 0.555 W/mK at 0.24% cobalt concentration at 30^0C, showing a 5.5% to 13.8% improvement in thermal conductivity when compared to base fluid. Cobalt nanofluids in 30:70 G/W base fluid offer exceptional thermal conductivity augmentation concerning cobalt particle concentration and temperature, as evidenced by the measured thermal conductivity values. The rise in the thermal conductivity of

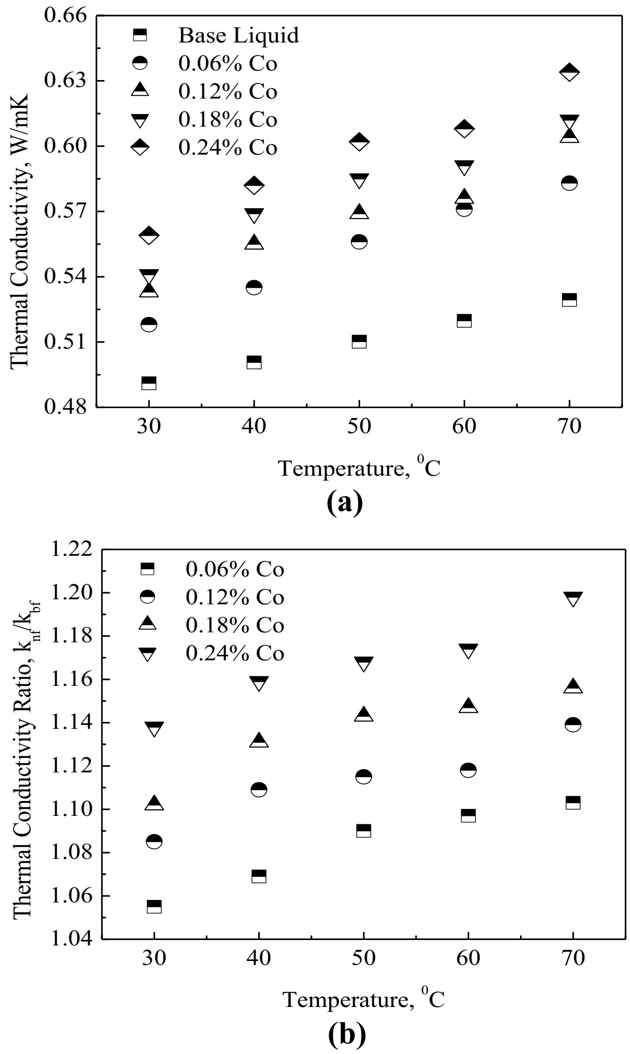

Fig. 6 Variation of **a** Thermal Conductivity and **b** Thermal Conductivity Ratio with Temperature

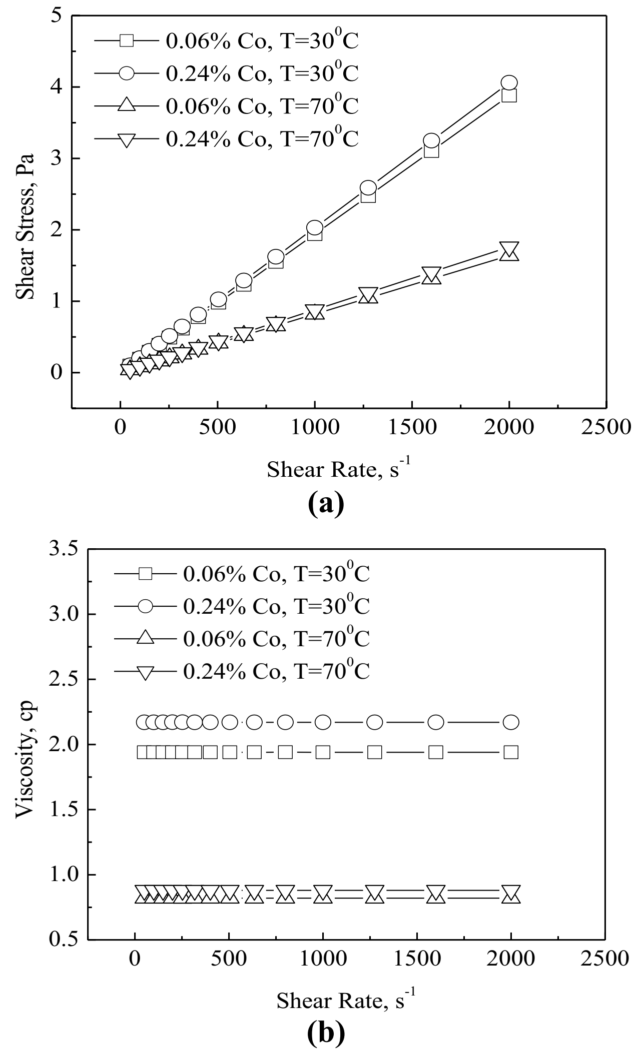

Fig. 7 Variation of **a** shear stress and **b** viscosity with shear rate

nanofluids with temperature is due to upraised Brownian motion, which depends on the temperature of the suspension [15]. The improvement in thermal conductivity with concentration can be due to the collective effect of Brownian motion, particle aggregation and development of sub-micron layer at particle surface [42].

3.4 Rheology and viscosity of cobalt nanofluids

3.4.1 Rheological behavior

The rheology and viscosities of the produced cobalt nanofluids were studied using a Brookfield digital rheometer model LVDV-III. The Brookfield Rheometer was used by previous researchers [15, 42] to examine the rheology and viscosity of nanofluids. Cobalt nanofluid rheology was undertaken to determine nanofluids' nature for the different concentrations. For a Newtonian fluid, the shear stress (τ) and shear rate (γ) are given by the well-known equation as shown below:

$$\tau = \mu\gamma \tag{4}$$

Figure 7(a) depicts the effect of shear rate on shear stress. Similarly, the impact of shear rate on viscosity is illustrated in Fig. 7(b). Figure 7(a) shows that shear stress varies linearly with the shear rate at all concentrations and temperatures of nanofluids. The range of shear rates considered is 0 to 2000s^{-1}. The viscosity remained unchanged at the same shear rate limits, as shown in Fig. 7(b). Hence, the cobalt nanofluids developed for this study behave like Newtonian fluids at all tested concentrations and temperatures.

3.4.2 Effect of temperature and concentration on viscosity

The viscosity variation of cobalt nanofluids with concentration and temperature are graphically represented in Fig. 8(a). The viscosities of cobalt nanofluids are more than base liquid and increase with concentration. Because of inter-linkages between dispersed particles and base liquid molecules, adding the cobalt nanoparticles to the base liquid enhances the mixture's viscosity. As the number of cobalt particles in the fluid increases, Vander Waal's forces between them cause to form larger nano-clusters. As a result of the restricted relative motion between the neighboring fluid layers in the dispersion, a more significant rise in viscosity was reported [42]. The viscosities of cobalt nanofluids decreased with a temperature rise. A similar trend in nanofluids concerning temperature and concentration is observed by previous researchers [8, 15]. The cobalt nanofluids have viscosities of 1.86cp and 2.17cp at 0% and 0.24% concentrations, respectively, suggesting a 4%and 16.3% increase in viscosity above base fluid at 30^{0}C. The viscosity of the nanofluids reduced from 2.17cp to 0.88cp for 30^{0}C and 70^{0}C for the maximum cobalt content of 0.24%. The values indicate that the nanofluids show a significant decrease in viscosity with temperature rise. Figure 8(b) shows a graphical representation of the viscosity ratio concerning temperature at various cobalt concentrations. As shown in Fig. 8(b), there are no significant fluctuations in viscosity ratio with temperature. As a result, GW30 based nanofluids are more favorable in heat transfer equipment as it requires constant pumping power.

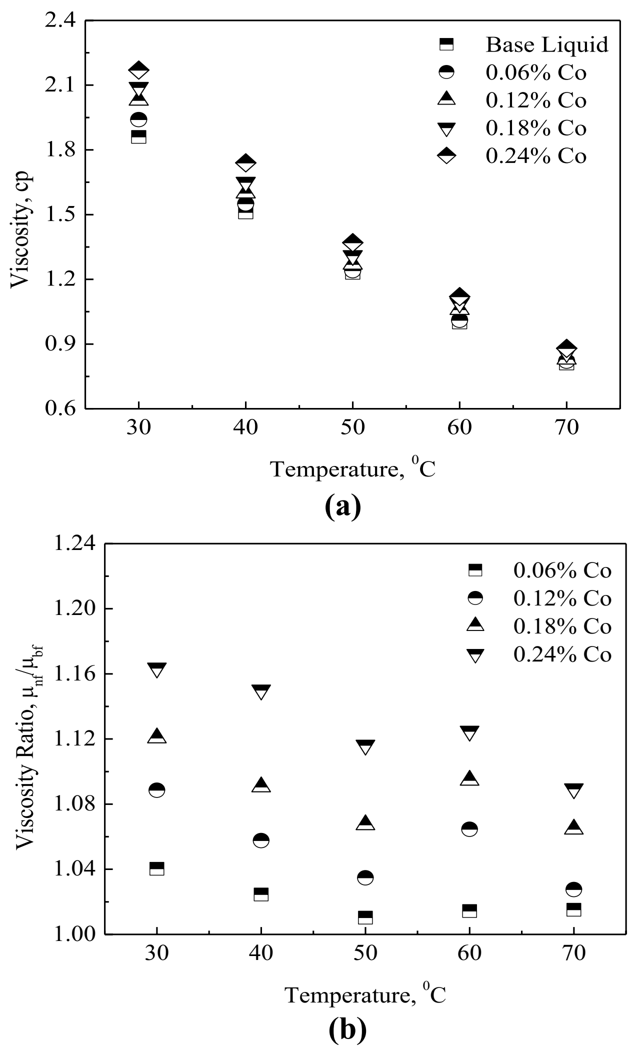

Fig. 8 Variation of **a** Viscosity and **b** Viscosity Ratio with Temperature

4 Development of regression correlations

Hamilton-Crosser [43], Batchelor [44], and Maxwell [45] proposed classical models for forecasting thermophysical and electrical properties; however, these models were not beneficial in estimating properties of produced Co nanofluids in this investigation. Few researchers attempted to alter the equations, while others attempted to build empirical models based on their experimental results. There are no comprehensive models for predicting properties, and existing models for predicting the nanofluid properties are limited to the type of nanoparticles and base liquids used and their operating range [26, 46]. Many investigators attempted to bring the experimental data together and develop thorough models for predicting nanofluid characteristics. To develop nanofluid property prediction models, some researchers used computer-based techniques such as artificial neural networks (ANN), genetic algorithms (GA.), fuzzy C-means clustering-based adaptive neuro-fuzzy system (FCM-ANFIS), group method of data handling (GMDH), least-square support vector machine (LSSVM) modeling, and machine learning algorithms [47].

In the subject of nanofluids, a great deal of experimental work is required to produce precise and vast quantities of property data that may be used to create more useful empirical models. However, experience has shown that the available models are ineffective for a variety of nanofluids. Lack of appropriate data, inaccuracy of available data, non-compliance of surfactant impacts on characteristics, and failure to account for the effect of microscopic nanoparticle features such as clustering, collision, and charge distribution are all reasons why established models are not applicable [26]. Regression equations are developed to analyze prepared Co nanofluid's viscosity, electrical, and thermal conductivities in this investigation. The regression equations work for Co nanofluids with an average particle size of 80 nm, volume concentrations ranging from 0.06% to 0.24%, and temperatures from 30 to 70^{0}C.The regression equations found are in terms of the variables that influence the specific property. The precision of the regression

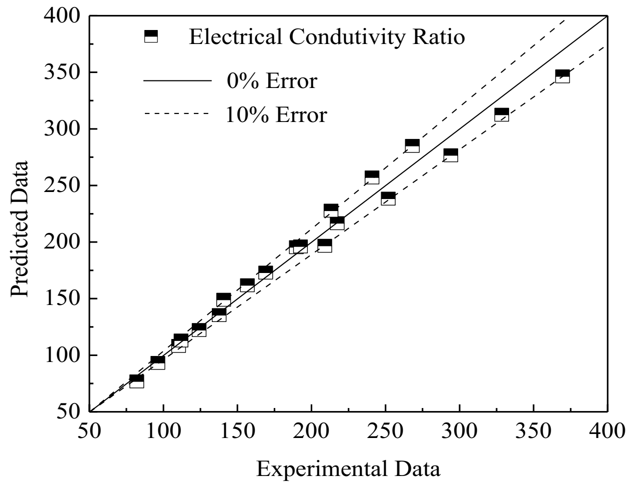

Fig. 9 Comparison of measured electrical conductivity with regression data

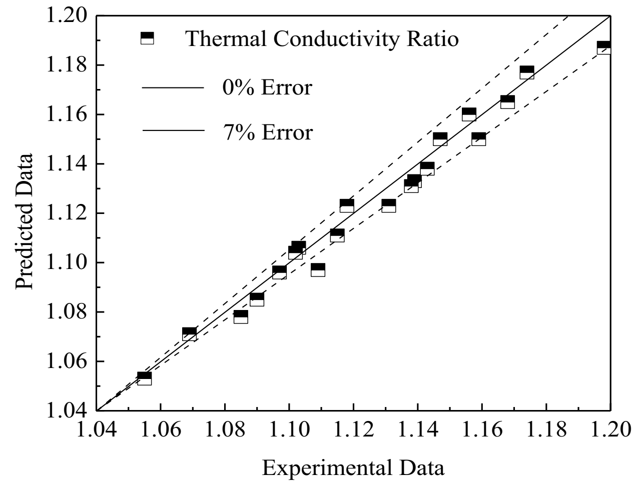

Fig. 10 Agreement between experimental and predicted data of thermal conductivity

equations is tested by comparing predicted data to experimental data, as shown in Figs. 9, 10 and 11. The most considerable percentage difference between projected and experimental data was between -10 and 10%. Below are the regression equations for electrical conductivity, thermal conductivity, and viscosity, respectively.

$$\sigma_R = \frac{\sigma_{nf}}{\sigma_{bf}} = 910.8T_R^{0.668}{\phi_R}^{0.6774} \tag{5}$$

$$k_R = \frac{k_{nf}}{k_{bf}} = 1.05T_R^{0.0609}(1+\phi_R)^{39.44}\left(1+d_{pR}\right)^{-0.2195}\left(1+\frac{\alpha_p}{\alpha_{bf}}\right)^{0.03812} \tag{6}$$

$$\mu_R = \frac{\mu_{nf}}{\mu_{bf}} = 0.9794T_R^{-0.0436}(1+\phi_R)^{53.21}\left(1+d_{pR}\right)^{-0.01519} \tag{7}$$

where, $T_R = \frac{T}{80}, \phi_R = \frac{\phi}{100}, d_{pR} = \frac{d_p}{80}$

The measured properties of the synthesized Co nanofluids could not be compared to similar findings in the literature due to a lack of comparable reports in the literature. As a result, the predicted thermal conductivity and viscosity data from the regressed equations at prepared concentrations and 30^0C is compared to data estimated from classical and generalized models provided by other researchers.

The classic model used to compare predicted thermal conductivity in this study is Hamilton and Crosser's [43] correlation. The equation proposed by Hamilton and Crosser is

$$k_R = \frac{k_{nf}}{k_{bf}} = \frac{k_p + (n-1)k_{bf} - (n-1)(k_{bf} - k_p)\phi}{k_p + (n-1)k_{bf} + (k_{bf} - k_p)\phi} \tag{8}$$

In Eq. (8), k_{nf} represents nanofluid thermal conductivity, k_p represents particle thermal conductivity, k_{bf} represents the base fluid thermal conductivity, and ϕ represents particle volume fraction. In the above equation, n = 3 for spherical particles.

Batchelor's classical model [44] is compared to the data predicted in the present study. The equation proposed by Batchelor is given by

$$\mu_R = \frac{\mu_{nf}}{\mu_{bf}} = 1 + 2.5\phi + 6.5\phi^2 \tag{9}$$

The mixture of the base fluid and suspended solids was assumed to be the anisotropic and homogeneous medium by Landau and Lifshitz [48], and the power value (n) in the mixing rule [49] was set to 1/3. The equation reported by Landau and Lifshitz to predict thermal conductivity is

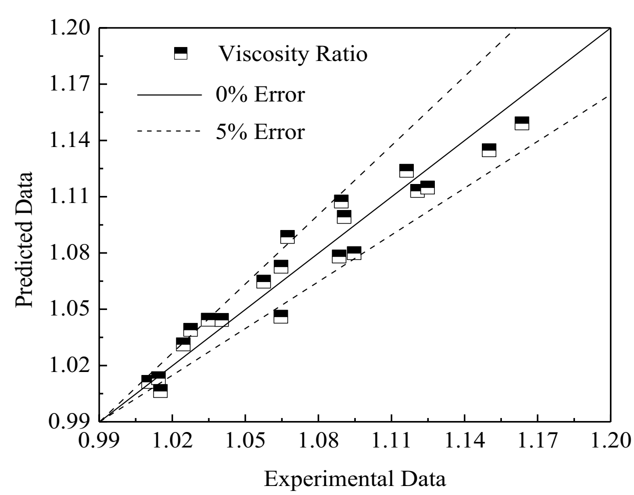

Fig. 11 Agreement between experimental and predicted data of thermal conductivity

$$k_R = \frac{k_{nf}}{k_{bf}} = \left((1-\phi)k_{bf}^{1/3} + \phi {k_p}^{1/3}\right)^3 \quad (10)$$

Hassani et al. [50] built a generalized empirical correlation for k_R using dimensional analysis between different π-groups, as indicated in the equation below

$$k_R = \pi_1 = 1.04 + \pi_2^{1.11}\pi_3^{0.33}\pi_4^{-1.7}\left[\frac{1}{\pi_4^{-1.7}} - \frac{262}{\pi_3^{0.33}} + \left(135\pi_5^{0.23}\pi_6^{0.82}\pi_7^{-0.1}\pi_8^{-7}\right)\right] \quad (11)$$

In the above equation $\pi_1 = k_{nf}/k_{bf}$, $\pi_2 = \phi$, $\pi_3 = k_{np}/k_{bf}$, $\pi_4 = Pr$, $\pi_5 = d_{ref}/d_p$, $\pi_6 = \nu_{bf}/d_p\upsilon_{Br}$, $\pi_7 = cp/T_1^{-1}\upsilon_{Br}^2$, $\pi_8 = T_{1b}$, υ_{Br} = Brownian velocity = $(18\kappa_b T_1/\pi\rho_p d_p^3)^{0.5}$, κ_b = Boltzmann constant = 1.3807×10^{-23} J/K.

Corcione [51] developed equations for thermal conductivity and viscosity ratios from a wide range of experimental data relating to nanofluids made up of metal and oxide nanoparticles with diameters ranging from 10 to 150 nm suspended in water or ethylene glycol using regression analysis. The equations proposed by Corcione are given as

$$k_R = \frac{k_{nf}}{k_{bf}} = 1 + 4.4Re^{0.4}\left(\frac{T_1}{T_{fr}}\right)^{10}\left(\frac{k_p}{k_{bf}}\right)^{0.03}\phi^{0.66} \quad (12)$$

$$\mu_R = \frac{\mu_{nf}}{\mu_{bf}} = \frac{1}{1 - 34.87\left(\frac{d_p}{d_f}\right)^{-0.3}\phi^{1.03}} \quad (13)$$

In the above equations, Re is the nanoparticle Reynolds number, Pr is the base liquid's Prandtl number, T_1 is the nanofluid temperature, and T_{fr} is the base liquid's freezing point. Reynolds number of nanoparticle is calculated by equation $Re = 2\rho_{bf}k_{bf}T_1/\pi\mu_f^2 d_p$. The equivalent diameter of a base fluid molecule $d_f = 0.1(6\ M/N\pi\rho_{f0})^{0.333}$, where M is the base fluid's molecular mass, N is the Avogadro number = 6.022×10^{23} mol^{-1}, and ρ_{f0} is the base liquid's density estimated at $T_0 = 293$ K.

Like Corcione [51], another researcher, Garoosi [52], proposed a generalized empirical equation based on regression analysis for thermal conductivity and viscosity ratios, but with more data and increased variance in particle and liquid base materials. The correlation derived by Garoosi is given as

$$k_R = \frac{k_{nf}}{k_{bf}} = \frac{k_p + 2k_{bf} + 2(k_p - k_{bf})\phi}{k_p + 2k_{bf} - (k_p - k_{bf})\omega\phi} + 3.762\left(\frac{T_1}{T_0}\right)^{8.661}\left(\frac{d_p}{d_f}\right)^{-0.4351}\left(\frac{k_p}{k_{bf}}\right)^{0.08235}\phi^{0.64}e^{-5.742\phi} \quad (14)$$

$$\mu_R = \frac{\mu_{nf}}{\mu_{bf}} = 1 + 49.6\left(\frac{d_p}{d_f}\right)^{-0.414}\phi^{0.908}e^{10.8\phi} \quad (15)$$

where M and N are the base fluid's molecular weights and the Avogadro number, respectively, ω = correction factor = 1 + 0.8946ϕ and ρ_{f0} is the base fluid's mass density estimated at $T_0 = 293$ K.

Moghaddam et al. [53] collected data on metal and metal oxide nanofluids from the literature to create and generate the regression correlation of thermal conductivity. In order to establish a new thermal conductivity correlation, 472 experimental data were collected, and all of them were incorporated in the regression analysis. The new correlation generated is presented below.

$$k_R = \frac{k_{nf}}{k_{bf}} = 1.0139\left(1 + \frac{\phi}{100}\right)^{2.964}\left(1 + \frac{T}{70}\right)^{0.155}\left(1 + \frac{d_p}{0.0275}\right)^{-0.01} \quad (16)$$

$$\mu_R = \frac{\mu_{nf}}{\mu_{bf}} = 1.1015\left(1 + \frac{\phi}{100}\right)^{9.053}\left(1 + \frac{T}{70}\right)^{0.095}\left(1 + \frac{d_p}{0.0275}\right)^{-0.027} \quad (17)$$

Udawattha et al. [54] defined the general viscosity ratio of nanofluids as a mix of static and dynamic components. The static part depicts the viscosity of composites or mixtures, whereas the active part depicts the effectual viscosity due to Brownian motion. The proposed equation is as follows:

$$\mu_R = \frac{\mu_{nf}}{\mu_{bf}} = \{Static\ part\} + \{Dynamic\ part\} = \{1 + 2.5\phi\} + \left\{\frac{\rho_p \upsilon_{Br} d_p^2}{72\delta\left[T \times 10^{-10} \times \phi^{-0.002T - 0.284}\right]}\right\} \quad (18)$$

where δ = distance between nanoparticles = $(\Pi d_p^3/6\phi)^{0.333}$.

Figure 12 compares the thermal conductivity predicted by the developed correlation in this study to generalized equations presented by other researchers. The thermal conductivity projected by the developed correlation in this work is much higher than the data projected by Hamilton and Crosser's [45] classical model. The disparity between the tested thermal conductivity ratio and the values estimated by theoretical equations is shown in Fig. 12. The discrepancy between measured thermal conductivity values and equation-predicted values is because equations do not account for the influence of the random motion of particles, which promotes energy transmission. Brownian movement is inhibited by nanoparticle aggregation, which is always present in nanofluids. The thermal conductivity of freshly

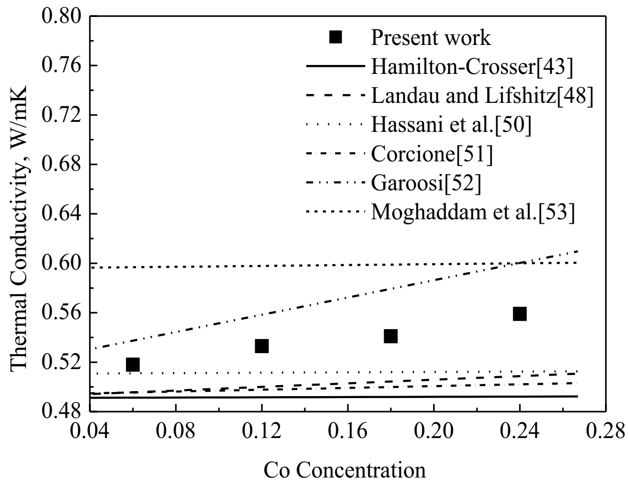

Fig. 12 Comparison between predicted thermal conductivity data in this study with other generalized correlations

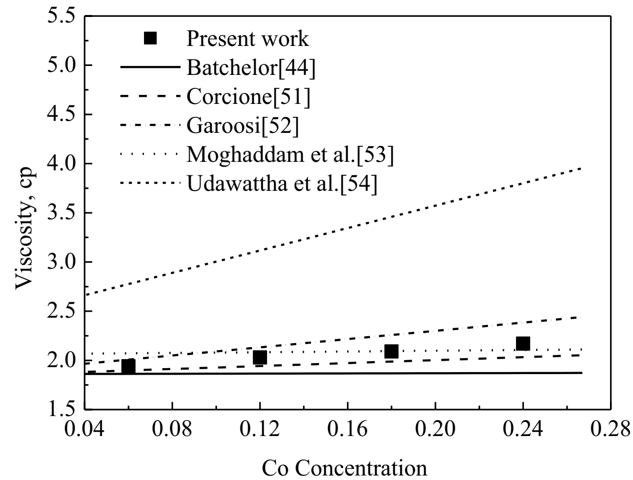

Fig. 13 Comparison between predicted viscosity data in this study with other generalized correlations

sonicated nanofluids with equally distributed nanoparticles is higher than the theoretical calculations anticipated [15]. Hassani et al. [50] and Garoosi [52] provided correlations that predicted data with a smaller margin, while the other correlations predicted data with a significant deviation. The largest deviation discovered between the results projected in this analysis and those predicted by Hassani et al. [50] and Garoosi [52] is 8% and 7%, respectively. Other generalized correlations reported by researchers [48, 51, 53] were unable to effectively forecast the data, which might be attributed to non-compliance with surfactant impacts on properties, as well as failing to account for the effect of tiny nanoparticle traits such as clustering, collision, and charge distribution [26].

The difference between the data estimated by classical and generalized models from literature and the projected viscosity via correlation proposed in this work is displayed in Fig. 13. In this study, the projected viscosity values are much higher than those predicted by Batchelor's [44] classical model. The concept of molecular bond weakening can explain the considerable difference in projected viscosities using classical models. Bond weakening is not considered in the classical models, and a similar argument has been made in the literature [46]. Corcione [51], Garoosi [52], and Moghaddam et al. [53] presented correlations that predicted the viscosity data of produced Co nanofluids with a smaller margin, while the other correlations [54] predicted data with a considerable divergence. The difference between the projected and predicted values by Udawattha et al. [54] was revealed to be as high as 42%. In contrast, the variation with correlations reported by other researchers [51–53] is less than 9%.

The nanofluid electrical conductivities can be estimated using the concept of Effective-Medium Theory (EMT). By applying EMT, Maxwell [45] generated a classical model to assess the electrical conductivities of bi-phase suspensions like nanofluids. Because there are no generalized correlations available for predicting the electrical conductivity of nanofluids in the literature, the electrical conductivity measured in this study was compared to relevant data provided by other researchers and classical models. This correlation is developed based on assumptions like homogeneous nanofluid, spherical morphology of the particles, non-interacting particles and low concentrations. The correlation proposed is formulated as follows:

$$\sigma_R = \frac{\sigma_{nf}}{\sigma_{bf}} = 1 + \frac{3\left(\frac{\sigma_p}{\sigma_{bf}} - 1\right)\phi}{\left(\frac{\sigma_p}{\sigma_{bf}} + 2\right) - \left(\frac{\sigma_p}{\sigma_{bf}} - 1\right)\phi} \tag{19}$$

In the above relation, ϕ represents volume concentration and σ_{nf}, σ_p and σ_{bf} are the electrical conductivities of the nanofluid, Nanoparticle and base material, respectively. Figure 14 depicts the disparity between experimental electrical conductivity, prediction from classical models and similar results published by other researchers [55, 56]. By large percentages, classical models underestimated the data. The omission of critical factors such as electrical double layer interactions, ion concentration, and particle clustering from classical models may result in significant discrepancies between experimental and theoretical data [12]. Because the electrical conductivity of 30:70 G/W based Co nanofluids is unknown in the literature, the measured data is compared to W-based Ag nanofluid's [55] and E.G. based Cu nanofluid's

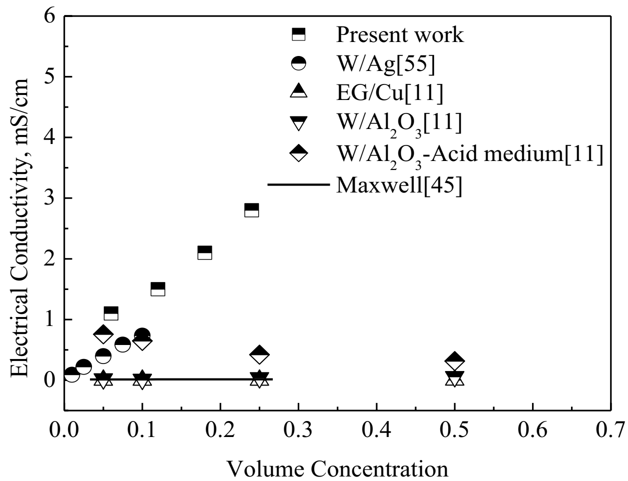

Fig. 14 Comparison between electrical conductivity data in this study with other reports

[11] electrical conductivities. The comparison is carried out at a temperature of 30^0C. The observed electrical conductivities of Co nanofluids are higher than those of Ag nanofluids and Cu nanofluids, as shown in Fig. 14. It could be because the nanofluids in this investigation were mixed with a highly concentrated HCl solution to change the pH. The surface conductance of the particle and the effective electrical conductivity of nanofluids rise when electrolytes are introduced to them [11]. Sarojini et al. [11] demonstrated that raising the electrolyte content increases the electrical conductivities of W based Al_2O_3 nanofluids, as seen in Fig. 14.

5 Heat transfer merit

The influence of nanofluid properties on heat transfer effectiveness can be predicted with the Mouromtseff correlation given by:

$$Mo = \frac{\rho^{0.8} k^{0.67} C^{0.33}}{\mu^{0.4}} \tag{20}$$

The proportion Mo_{nf}/Mo_{bf}, also known as the Mouromtseff ratio, is a performance criterion for nanofluids. The nanofluid is more suited for heat transfer operations if the Mo ratios are more significant than unity [56]. The values of nanofluid specific heat and density in the Mouromtseff correlation can be calculated using the rule of mixtures [57]. Table 7 shows that the Mouromtseff ratio for cobalt nanofluids is more than one ($Mo > 1$) at all concentrations. So, when operated under turbulent range, the cobalt nanofluids exhibit a better heat transfer gain than the 30:70 G/W base fluid.The more considerable rise in thermal conductivity of nanofluids, which is not shielded by a commensurate increase in their viscosity, can be attributed to the rationalization of this fact.

6 Uncertainty in property measurement

The experimental approaches for estimating material properties are invariably coupled with measurement errors. The precision of the instruments used is considered when evaluating uncertainties in the measured data. The accuracy of the electrical conductivity gauge, KD2 Pro and the Viscometer is ± 1%, as specified by the manufacturers. The temperature bath utilized in the constant temperature maintenance and the electronic weighing equipment used to measure nanoparticle weight is 0.01gms and 0.1^0C, respectively.

The uncertainty in measuring thermal conductivity and viscosity is evaluated by the relations reported by Teng et al. [58] and Prasad et al. [59], which are given by

$$U_\sigma = \pm\sqrt{\left(\frac{\Delta\sigma}{\sigma}\right)^2 + \left(\frac{\Delta w}{w}\right)^2 + \left(\frac{\Delta T}{T}\right)^2} \tag{21}$$

$$U_k = \pm\sqrt{\left(\frac{\Delta k}{k}\right)^2 + \left(\frac{\Delta w}{w}\right)^2 + \left(\frac{\Delta T}{T}\right)^2} \tag{22}$$

$$U_\mu = \pm\sqrt{\left(\frac{\Delta\mu}{\mu}\right)^2 + \left(\frac{\Delta w}{w}\right)^2 + \left(\frac{\Delta T}{T}\right)^2} \tag{23}$$

In above equations, σ, k, w, and T are measured data, and Δσ, Δk, Δμ, Δw and ΔT are measurement accuracies of thermal conductivity, viscosity, nanoparticle weight, and temperatures, respectively, in the relations as mentioned earlier. The above relationships were utilized to determine the uncertainties in property measurements and found a maximum of 2.26% uncertainty.

Table 7 Mouromtseff ratio of cobalt nanofluids

Volume Percentage	Density (kg/m.^{3})	Specific heat (J/kg·K)	Thermal conductivity (W/m·K)	Viscosity (mPa·s)	Mo Ratio
0	1078	3566.36	0.491	1.86	1
0.06	1083	3548.851	0.518	1.94	1.02108
0.12	1087	3531.492	0.533	2.03	1.02395
0.18	1092	3514.282	0.541	2.09	1.0241
0.24	1097	3497.218	0.559	2.17	1.03306

7 Conclusions

The present work addresses the dispersion stability of nanofluid by selecting an ideal base liquid mixture. The work compares the relative advantages of Glycerol/Water blends as base fluid at various percentage weight concentrations of Glycerol. The increase in Glycerol percentage in mix enhances the viscosity and diminishes thermal conductivity. The 30:70 G/W is selected as the best choice for producing cobalt nanofluids. The prepared cobalt nanofluids were stable even after 50 days from the day of preparation. FESEM analysis was used to determine the particle morphology and suspension stability of cobalt suspensions in 30:70 G/W mixture. The uniformity in measured data of Electrical conductivity and Zeta potential over 50 days further confirms the stability. The electrical and thermal conductivities of cobalt nanofluids increase with concentration and temperature. Cobalt nanofluid's viscosities rise with concentration and fall with temperature. The maximum improvement in nanofluid's electrical and thermal conductivities is found to be 340 times and19.8% at a temperature of 70^0C, respectively, for the maximum cobalt nanofluid concentration of 0.24%. The maximum enhancement in cobalt nanofluid's viscosity is determined to be 16.3% at a temperature of 30^0C with 0.24% cobalt concentration. Regression equations are developed to estimate cobalt nanofluid's electrical conductivity, thermal conductivity, and viscosity. The Mouromtseff ratio for cobalt nanofluids is more than one, indicating these nanofluids has good effectiveness for thermal transport in turbulent flow.

Acknowledgements The authors acknowledge the permission of the Center for Energy Studies, JNTUH College of Engineering, Hyderabad, to undertake experiments. The authors would like to express their gratitude to the Department of Chemistry, JNTUH for allowing us to utilize the equipment to prepare nanofluids. No financial support is received by the authors to undertake the present work.

Declarations

Conflict of interests The authors hereby declare that there are no known competing financial interests or personal connections that could have influenced the study's conclusions. The authors did not receive support from any organization for the submitted work.

References

1. Das SK, Putra N, Thiesen P, Roetzel W (2003) Temperature Dependence of Thermal Conductivity Enhancement for Nanofluids. J Heat Transfer 125:567–574. https://doi.org/10.1115/1.1571080
2. Li CH, Peterson GP (2007) Mixing effect on enhancing the effective thermal conductivity of nanoparticle suspensions (nanofluids). Int J of Heat and Mass Transfer 50:4668–4677. https://doi.org/10.1016/j.ijheatmasstransfer.2007.03.015
3. Khodadadi H, Aghakhani S, Majd H, Kalbasi R, Wongwises S, Afrand M (2018) A comprehensive review on the rheological behavior of mono and hybrid nanofluids: Effective parameters and predictive correlations. Int J Heat Mass Transf 127:997–1012. https://doi.org/10.1016/j.ijheatmasstransfer.2018.07.103
4. Koca HD, Doganay S, Turgut A, Tavman IH, Saidur R, Mahbubul IM (2018) Effect of particle size on the viscosity of nanofluids: A review. Renew Sustain Energy Rev 82:1664–1674. https://doi.org/10.1016/j.rser.2017.07.016
5. Li XF, Zhu DS, Wang XJ, Wang N, Gao JW, Li H (2008) Thermal conductivity enhancement dependent pH and chemical surfactant for Cu-H_2O nanofluids. Thermochim Acta 469:98–103. https://doi.org/10.1016/j.tca.2008.01.008
6. Hemmat Esfe M, Saedodin S, Wongwises S, Toghraie D (2015) An experimental study on the effect of diameter on thermal conductivity and dynamic viscosity of Fe/water nanofluid. J Therm Anal Calorim 119:1817. https://doi.org/10.1007/s10973-014-4328-8
7. Ghosh MM, Ghosh S, Pabi SK (2012) On Synthesis of a Highly Effective and Stable Silver Nanofluid Inspired by Its Multiscale Modelling. Nanosci Nanotechnol Lett 4:1–6. https://doi.org/10.1166/nnl.2012.1392
8. Paul G, Pal T, Manna I (2010) Thermophysical property measurement of nano-gold dispersed water-based nanofluids prepared by chemical precipitation technique. J Colloid Interface Sci 349:434–437. https://doi.org/10.1016/j.jcis.2010.05.086
9. Kim HJ, Bang IC, Onoe J (2009) Characteristic stability of bare Au-water nanofluids fabricated by pulsed laser ablation in liquids. Opt Lasers Eng 47:532–538. https://doi.org/10.1016/j.optlaseng.2008.10.011
10. Shalkevich N, Escher W, Burgi T, Michel B, Si-Ahmed L, Poulikakos D (2010) On the Thermal Conductivity of Gold Nanoparticle Colloids. Langmuir 26(2):663–670. https://doi.org/10.1021/la9022757
11. Sarojini KK, Manoj SV, Singh PK, Pradeep T, Das SK (2013) Electrical conductivity of ceramic and metallic nanofluids. Colloids Surf A Physicochem Eng Asp 417:39– 46. https://doi.org/10.1016/j.colsurfa.2012.10.010
12. Konakanchi H, Vajjha R, Misra D, Das D (2011) Electrical Conductivity Measurements of Nanofluids and Development of New Correlations. J Nanosci Nanotechnol 11:1–8. https://doi.org/10.1166/jnn.2011.4217
13. Fan Yu, Chen Y, Liang X, Xu J, Lee C, Liang Q, Tao P, Deng T (2017) JialeXu, Chiahsun Lee, Qi Liang, PengTao and Tao Deng, Dispersion stability of thermal nanofluids. Prog Nat Sci 27(5):531–542. https://doi.org/10.1016/j.pnsc.2017.08.010
14. Pagliaro M (2017) Glycerol: The Renewable Platform Chemical. Elsevier Publications, Amsterdam, The Netherlands
15. Akilu S, Baheta AT, Minea AA, Sharma KV (2017) Rheology and thermal conductivity of non-porous silica (SiO_2) in viscous glycerol and ethylene glycol-based nanofluids. Int Commun Heat Mass Transf 88:245–253. https://doi.org/10.1016/j.icheatmasstransfer.2017.08.001
16. Akilu S, Sharma KV, Aklilu TB, Azman MM, Bhaskoro PT (2016) Temperature-Dependent Properties of Silicon Carbide Nanofluid in Binary Mixtures of Glycerol-Ethylene Glycol. Procedia Eng 148:774–778. https://doi.org/10.1016/j.proeng.2016.06.555
17. Tshimanga N, Sharifpur M, Meyer JP (2016) Experimental investigation and model development for thermal conductivity of glycerol MgO nanofluids. Heat Transfer Eng 37(18):1538–1553. https://doi.org/10.1080/01457632.2016.1151297
18. Ijam A, Moradi Golsheikh A, Saidur R, Ganesan P (2014) A glycerol–water-based nanofluid containing graphene oxide nanosheets. J Mater Sci 49(17):5934–5944. https://doi.org/10.1007/s10853-014-8312-2
19. Sharifpur M, Tshimanga N, Meyer JP, Manca O (2017) Experimental investigation and model development for thermal conductivity

of α-Al_2O_3-glycerol nanofluids. Int Commun Heat Mass Transfer 85:12–22. https://doi.org/10.1016/j.icheatmasstransfer.2017.04.001
20. Sharifpur M, Adio SA, Meyer JP (2015) Experimental investigation and model development for effective viscosity of Al_2O_3–glycerol nanofluids by using dimensional analysis and GMDH-NN methods. Int Commun Heat Mass Transfer 68:208–219. https://doi.org/10.1016/j.icheatmasstransfer.2015.09.002
21. Abareshi M, Sajjadi SH, Zebarjad SM, Goharshadi EK (2016) Fabrication, characterization, and measurement of viscosity of α-Fe_2O_3-glycerol nanofluids. J Mol Liq 163:27–32. https://doi.org/10.1016/j.molliq.2011.07.007
22. Pak BC, Cho YI (1998) Hydrodynamic and heat transfer study of dispersed fluids with submicron metallic oxide particles. Exp Heat Transfer 11:151–170. https://doi.org/10.1080/08916159808946559
23. Moita A, Moreira A, Pereira J (2021) Nanofluids for the Next Generation Thermal Management of Electronics: A Review. Symmetry 13:1362. https://doi.org/10.3390/sym13081362
24. Escher W, Brunschwiler T, Shalkevich N, Shalkevich A, Burgi T, Michel B, Poulikakos D (2011) On the Cooling of Electronics With Nanofluids, ASME. J Heat Transfer 133(5):051401. https://doi.org/10.1115/1.4003283
25. Hatami N, Banari AK, Malekzadeh A, Pouranfard AR (2017) The effect of magnetic field on nanofluids heat transfer through a uniformly heated horizontal tube. Phys Lett A 381(5):510–515. https://doi.org/10.1016/j.physleta.2016.12.017
26. Yang L, Jianyong Xu, Kai Du, Zhang X (2017) Recent developments on viscosity and thermal conductivity of nanofluids. Powder Technol 317:348–369. https://doi.org/10.1016/j.powtec.2017.04.061
27. Cheng NS (2008) Formula for the viscosity of the glycerol-water mixture. Ind Eng Chem Res 47:3285–3288. https://doi.org/10.1021/ie071349z
28. Bates OK (1936) Binary Mixtures of Water and Glycerol - Thermal Conductivity of Liquids. Ind Eng Chem 28(4):494–498. https://doi.org/10.1021/ie50316a033
29. Jamshidi N, Farhadi M, Ganji DD, Sedighi K (2012) Experimental investigation on the viscosity of nanofluids. IJE Trans B: Appl 25:201–210. https://doi.org/10.5829/idosi.ije.2012.25.03b.07
30. Ghadimi A, Saidur R, Metselaar HS (2011) A review of nanofluid stability properties and characterization in stationary conditions. International Journal of Heat and Mass Transfer 54:4051–4068. https://doi.org/10.1016/j.ijheatmasstransfer.2011.04.014
31. Suseel Jai Krishnan S, Nagarajan PK (2019) Influence of stability and particle shape effects for an entropy generation based optimized selection of magnesia nanofluid for convective heat flow applications. Appl Surf Sci 489:560–575. https://doi.org/10.1016/j.apsusc.2019.06.038
32. Choudhary R, Khurana D, Kumar A, Subudhi S (2017) Stability analysis of Al_2O_3/water nanofluids. J Exp Nanosci 12(1):40–151. https://doi.org/10.1080/17458080.2017.1285445
33. Hwang Y, Lee J-K, Lee J-K, Jeong Y-M, Cheong S-i, Ahn Y-C, Kim SH (2008) Production and dispersion stability of nanoparticles in nanofluids. Powder Technol 186:145–153. https://doi.org/10.1016/j.powtec.2007.11.020
34. Kumar MS, Vasu V, Gopal AV (2016) Thermal conductivity and rheological studies for Cu–Zn hybrid Nanofluids with various base fluids. J Taiwan Inst Chem Eng 66:321–327. https://doi.org/10.1016/j.jtice.2016.05.033
35. David R (2003) Lide, CRC Handbook of Chemistry and Physics. CRC Press, Boca Raton, Florida
36. Babita, Sharma SK, Gupta SM (2016) Preparation and evaluation of stable nanofluids for heat transfer application: A review. Exp Therm Fluid Sci 79:202–212. https://doi.org/10.1016/j.expthermflusci.2016.06.029
37. Zawrah MF, Khattab RM, Girgis LG, El Daidamony H, Abdel Aziz RE (2014) Stability and electrical conductivity of water-based Al2O3 nanofluids for different applications. HBRC J 12(3):227–234. https://doi.org/10.1016/j.hbrcj.2014.12.001
38. Shoghl SN, Jamali J, Moraveji MK (2016) Electrical conductivity, viscosity, and density of different nanofluids: An experimental study. Exp Therm Fluid Sci 74:339–346. https://doi.org/10.1016/j.expthermflusci.2016.01.004
39. Minea AA, Luciu RS (2012) Investigations on the electrical conductivity of stabilized water-based Al_2O_3 nanofluids. Microfluid Nanofluid 13(6):977–985. https://doi.org/10.1007/s10404-012-1017-4
40. Baby TT, Ramaprabhu S (2010) Investigation of thermal and electrical conductivity of graphene-based nanofluids. J Appl Phys 108:124308. https://doi.org/10.1063/1.3516289
41. Sadri R, Ahmadi G, Togun H, Dahari M (2014) Salim Newaz Kazi, Emad Sadeghinezhad and Nashrul Zubir, An experimental study on thermal conductivity and viscosity of nanofluids containing carbon nanotubes. Nanoscale Res Lett 9:151. https://doi.org/10.1186/1556-276X-9-151
42. Akilu S, Baheta AT, Kadirgama K, Padmanabhan E, Sharma KV (2019) Viscosity, electrical and thermal conductivities of ethylene and propylene glycol-based β-SiC nanofluids. J Mol Liq 284:780–792. https://doi.org/10.1016/j.molliq.2019.03.159
43. Hamilton RL, Crosser OK (1962) Thermal conductivity of heterogeneous two-component systems. Ind Eng Chem Fundam 1:182–191. https://doi.org/10.1021/i160003a005
44. Batchelor GK (1977) The effect of Brownian motion on the bulk stress in a suspension of spherical particles. J Fluid Mech 83:97–117. https://doi.org/10.1017/S0022112077001062
45. Maxwell JC (1881) Treatise on Electricity and Magnetism, seconded. Clarendon Press, Oxford, U.K.
46. Porgar S, Vafajoo L, Nikkam N, Vakili-Nezhaad G (2021) A comprehensive investigation in the determination of nanofluids thermophysical properties. J Indian Chem Soc 98(3):100037. https://doi.org/10.1016/j.jics.2021.100037
47. Hemmati-Sarapardeh A, Varamesh A, Husein MM, Karan K (2018) On the evaluation of the viscosity of nanofluid systems: Modeling and data assessment. Renew Sustain Energy Rev 81(1):313–329. https://doi.org/10.1016/j.rser.2017.07.049
48. Landau LD, Lifshitz EM (1960) The propagation of electromagnetic waves. Electron Contin Media 8:290–330
49. Nan C-W (1993) Physics of inhomogeneous inorganic materials. Prog Mater Sci 37:1–116. https://doi.org/10.1016/0079-6425(93)90004-5
50. Hassani S, Saidur R, Mekhilef S, Hepbasli A (2015) A new correlation for predicting the thermal conductivity of nanofluids; using dimensional analysis. Int J Heat Mass Transf 90:121–130. https://doi.org/10.1016/j.ijheatmasstransfer.2015.06.040
51. Corcione M (2011) Empirical correlating equations for predicting the effective thermal conductivity and dynamic viscosity of nanofluids. Energy Convers Manage 52(1):789–793. https://doi.org/10.1016/j.enconman.2010.06.072
52. Garoosi F (2020) Presenting two new empirical models for calculating the effective dynamic viscosity and thermal conductivity of nanofluids. Powder Technol 366:788–820. https://doi.org/10.1016/j.powtec.2020.03.032
53. Moghaddam HA, Ghafouri A, Faridi Khouzestani R (2021) Viscosity and thermal conductivity correlations for various nanofluids based on different temperature and nanoparticle diameter. J Braz Soc Mech Sci Eng 43:303. https://doi.org/10.1007/s40430-021-03017-1
54. Udawattha DS, Narayana M, Wijayarathne UPL (2019) Predicting the effective viscosity of nanofluids based on the rheology of suspensions of solid particles. Journal of King Saud University – Science 31(3):412–426. https://doi.org/10.1016/j.jksus.2017.09.016
55. Heyhat MM, Irannezhad A (2018) Experimental investigation on the competition between enhancement of electrical and thermal

conductivities in water-based nanofluids. J Mol Liq 268:169–175. https://doi.org/10.1016/j.molliq.2018.07.022
56. Mouromtseff I (1942) Water and forced-air cooling of vacuum tubes nonelectronic problems in electronic tubes. Proc IRE 30:190–205. https://doi.org/10.1109/JRPROC.1942.234654
57. Azmi WH, Sharma KV, Sarma PK, Mamat R, Anuar S, Rao VD (2013) Experimental determination of turbulent forced convection heat transfer and friction factor with SiO_2 nanofluid. Exp Therm Fluid Sci 51:103–111. https://doi.org/10.1016/j.expthermflusci.2013.07.006
58. Teng TP, Hung YH, Teng TC, Mo HE, Hsu HG (2010) The effect of alumina/water nanofluid particle size on thermal conductivity. Appl Therm Eng 30(14):2213–2218. https://doi.org/10.1016/j.applthermaleng.2010.05.036
59. Prasad TR, Krishna KR, Sharma KV, Bhaskar CN (2022) Thermal performance of stable SiO2 nanofluids and regression correlations to estimate their thermophysical properties. J Indian Chem Soc 99(6):100461. https://doi.org/10.1016/j.jics.2022.100461